Black Hole Ring Images from PSF Structures

Makoto Miyoshi[1], Yoshiaki Kato[2], Junichiro Makino[3]

Abstract Two critical aspects of radio interferometric imaging analysis are the data calibration and deconvolution of the point spread function (PSF) structure. Both of these are particularly important for high-frequency observations using a VLBI network consisting of a small number of stations, such as those conducted by the Event Horizon Telescope (EHT). The Event Horizon Telescope Collaboration (EHTC) has presented images of ring-shaped black holes from observations of M 87 ($d = 42 \pm 3$ μas) [1] and the Galactic Center ($d = 51.8 \pm 2.3$ μas) [2]. The ring structures seen in the EHTC images are consistent with the estimated shadow diameter of the black hole based on its mass and distance. However, these black hole ring sizes are also the same with the typical up-and-down spacings (e.g., the intervals between the main beam and nearby sidelobes) seen in the point spread function (PSF; dirty beam) for each observation. These facts suggest that the EHTC ring structures are artifacts derived from the shape of the PSFs rather than the intrinsic structure of M 87 and the Galactic Center. The EHTC utilizes novel imaging techniques alongside the standard CLEAN algorithm. The CLEAN method was designed with PSF shape deconvolution in mind; yet, in practice, it may not always be able to completely remove the PSF shape. In the imaging analysis of data from interferometers with a small number of antennas like the EHT, it is crucial to assess the PSF shape and compare it with the imaging results. The novel imaging methods employed by the EHTC have not yet been fully evaluated for PSF deconvolution performance, and it is highly recommended that their performance in this regard be thoroughly examined. It is also important to scrutinize the data calibration capability, i.e., the ability to separate error noise from the observed data.

Keywords Imaging, Deconvolution, Point Spread Function, EHTC Ring Image

1 Principles of VLBI Imaging

Although VLBI imaging appears to use a different approach to data processing than optical/IR telescopes, the basic imaging principle is the same. That is, the resulting image is a convolution of the PSF of the telescope and the structure of the observed object (Figure 1). However, in the case of radio interferometry,

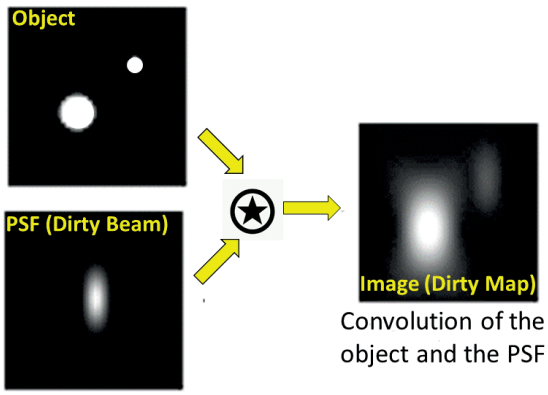

Fig. 1 The obtained observational image (dirty map) is a convolution of the PSF (dirty beam) of the observing instrument (telescope) with the brightness distribution of the source object. To get the object structure, we need to deconvolve the PSF structure from the dirty map.

1. National Astronomical Observatory Japan
2. Japan Meteorological Agency
3. Kobe University

where the spatial Fourier component cannot be adequately sampled (this is especially true for VLBI), the PSF structure is not sharp, so deconvolution of the PSF structure is necessary to clarify the object image. In other words, the imaging process in radio interferometry is the process of deconvolving the PSF of the array. In actual processing, it is difficult to completely remove the influence of the PSF structure, and it often occurs that the influence of the PSF structure may remain.

Here, using the EHTC black hole imaging results as a concrete example, we investigate the effects of the PSF structure, in particular their results for the Galactic Center. For more information on the independent analysis of the EHT Sgr A* data, see the paper [7].

2 The EHTC Black Hole Ring Images

We show that the shapes of the ring images of the EHTC are consistent with the features of its PSF structures.

2.1 The Main Beam Fits in the EHTC Rings

The influence of PSF is prominently observed in black hole imaging by the EHTC. As shown in Figure 2, the shape of the central hole in the ring image of Sgr A* reported by the paper [2] nearly matches the shape of the PSF's main beam. This suggests the possibility of incomplete deconvolution. Note that a similar situation was seen in the M 87 ring image by the EHTC [1].

2.2 Correspondence Between PSF Structure and Ring Image

As shown in Figure 3, examining the PSF structure from the EHT2017 Sgr A* observation data reveals a bumpy structure around the central main beam, with peaks and dips both spaced at 50 μas intervals.

This matches the diameter of the ring shown by the paper [2], indicating that the PSF structure significantly influences the imaging results. The PSFs for both observed sources show very bumpy structures.

The intensity of the first sidelobe is non-negligible with respect to the main beam, and a deep dip is present at their midpoints. The interval between the bumpy PSF structure is consistent with the diameter of the ring image obtained by the EHTC (Table 1).

We have also confirmed that it is possible to create rings that are very similar to the EHTC rings, even from simulated data that are not ring structures. Thus, the EHTC ring image can be considered to originate not from the observed source but from the PSF structure.

Table 1 Measurements of the EHTC rings and the characteristics of the corresponding PSFs. Predicted shadow sizes, measured ring diameters, and the restoring beam shapes are from EHTC papers. Default beam values are from April 11 for M 87 and April 7 for Sgr A*. The values of the PSF structures are from our measurements.

	M 87	Sgr A*
Predicted Shadow Size	$37.6^{+6.2}_{-3.5}$ or $21.3^{+5}_{-1.7}$ μas	~ 50 μas
EHTC Measurements		
$D_{\rm ring}$	42 ± 3 μas	51.8 ± 2.3 μas
$D_{\rm Shadow}$	-	48.7 ± 7.0 μas
EHT PSF Structure		
1st Sidelobe Position from the Main Beam	46 μas	49.09 μas
1st Sidelobe Intensity Relative to the Main Beam	+70%	+49%
Negative Minima at the Midpoint	−60%	−78.1%
Restoring Beam Shape		
Default		
FWHM$_{maj\times min}$	25.4 × 17.4 μas	23.0 × 15.3 μas
Position Angle	6.0°	66°
EHTC Used		
FWHM	20 μas	20 μas

2.3 EHTC Imaging Simulation Results

The EHTC used several image synthesis algorithms. As shown in Figure 4, the EHTC image synthesis simulation results from each method show bumpy structures with 50 μas intervals that are characteristic of the PSF structure. Even from model data that are not ring structures, there are examples of 50 μas rings or arc-like structures appearing in the resulting images. This suggests that none of the imaging methods used in the EHTC are able to fully deconvolve the effects of PSF structures.

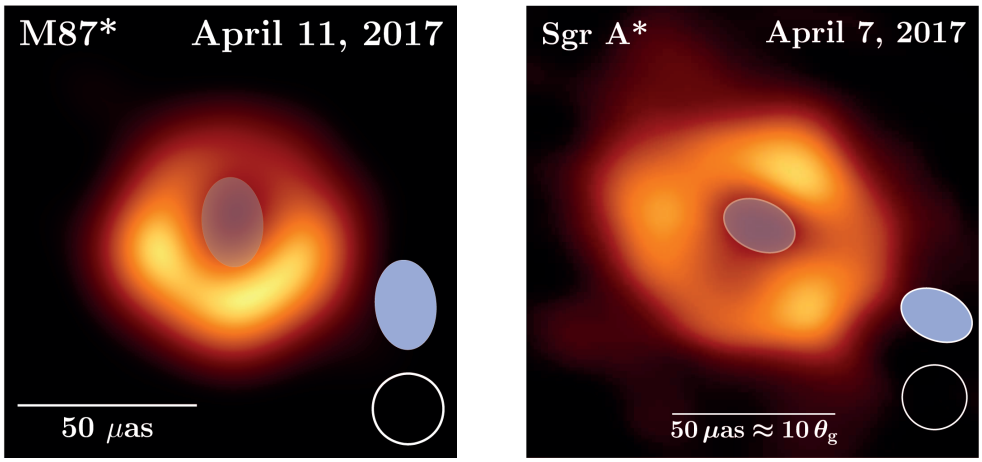

Fig. 2 Comparison of the default restoring beams and the EHTC images. The left panel shows the case of M 87. The default restoring beam is an ellipse with FWHM $= 25.0 \times 17.4$ μas and PA $= 6.0^\circ$, which is shown as a blue ellipse in the panel. The white circle shows the restoring beam used by the EHTC to make their images. The original image is taken from Figure 3 in the paper [1]. The right panel shows the case of Sgr A*. The default restoring beam is an ellipse with FWHM $= 23.0 \times 15.3$ μas and PA $= 66.6^\circ$, which is shown as a blue ellipse in the panel. The white circle shows the restoring beam used by the EHTC to make their images. The original image is taken from Figure 3 in the paper [2]. The size and shape of the default restoring beam is nearly the same as with the central shadow.

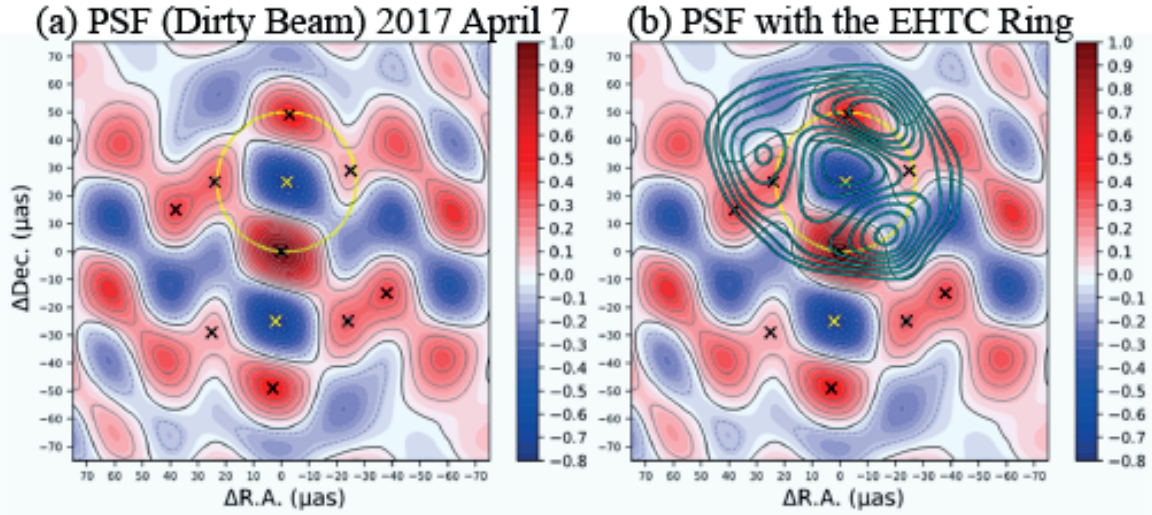

Fig. 3 The point spread function (dirty beam) of the EHT array (2017) on the second day of Sgr A* observations. In Panel (a), black x-marks represent the peak positions near the center, while yellow x-marks depict the deepest minimum positions. The yellow dotted line indicates the circle with a diameter of 50 μas centered at the deepest minimum (north) in the dirty beam. In Panel (b), we overlay the EHTC ring image (blue contour lines) on the dirty beam. The contour intervals of the EHTC ring image are set at every 10% of the peak value.

3 Conclusion

In VLBI imaging, deconvolution of the PSF structure and calibration of the data are crucial. Especially with a limited number of stations, the PSF structure strongly influences the resulting image, highlighting the need for accurate deconvolution. The EHT black hole imaging examples show the significant influence of the PSF on their images. Therefore, a detailed analysis of the PSF and its effects must be thoroughly considered in VLBI imaging.

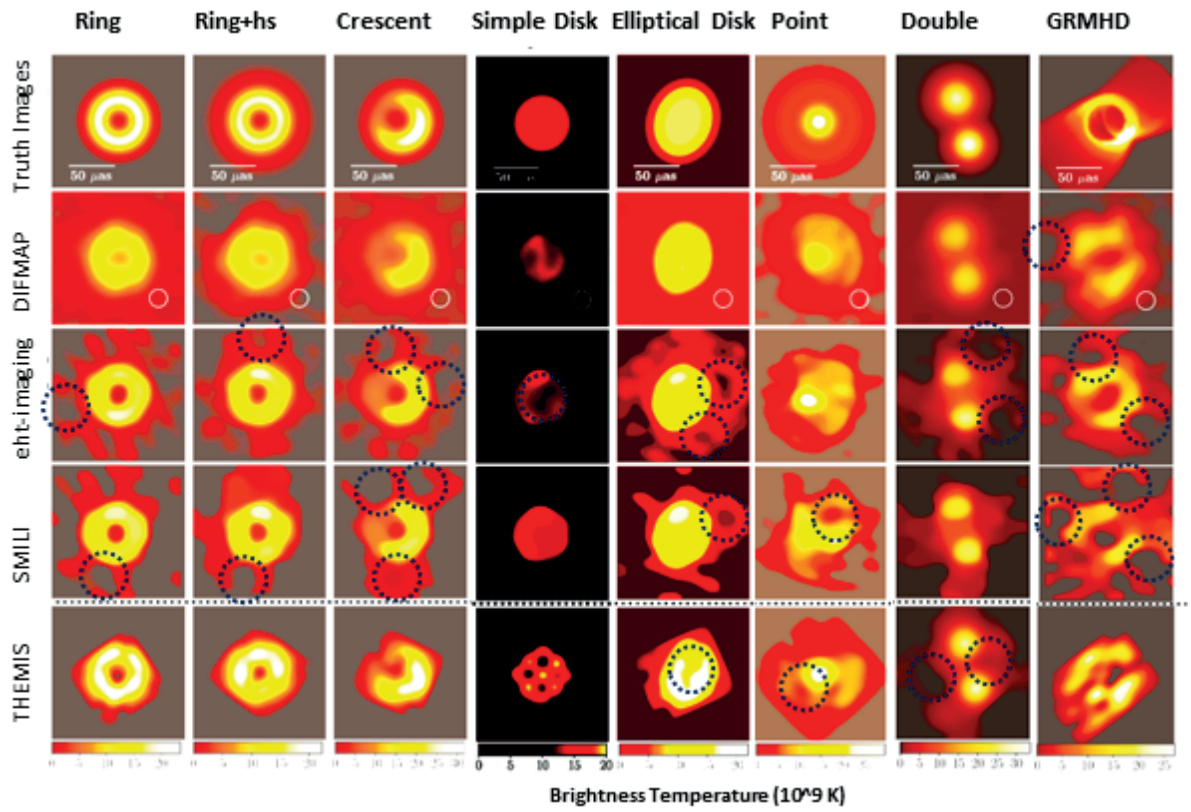

Fig. 4 Influence of PSF structure found on the EHTC imaging simulation results for Sgr A*. This figure is modified from Figure 11 (a) showing the EHTC image simulation results in the paper [3]. Its image brightness was adjusted for each model image. The black dotted circles have a diameter of 50 μas. Most of the imaging results show not only the given model image but also some things with an interval of about 50 μas. Some of them are ring-shaped with a diameter of 50 μas. Even from the non-ring image models (point, double point and flat brightness disks), the reconstructed images show ring-shaped structures of 50 μas diameter.

4 Note

In principle, we can change the shape of the PSF by changing the weighting of the data points, but not much in the case of sparse data sampling; in the M 87 and Sgr A* data of EHT2017, the separation between the first sidelobe and the main beam is almost unchanged, and the height of the sidelobes is also NOT negligible with respect to the main beam height (see, e.g., Figure 32 in the paper [4]).

The EHTC has made data from the first observations (2017) public at the same time as the publication of their paper. We thank the EHTC for this, which allowed us to conduct our independent investigation and analysis. We hope that all of the EHT polarimetric data and subsequent observational data will be made publicly available as soon as possible.

References

1. The Event Horizon Telescope Collaboration et al., 2019, ApJL, 875, L1
2. The Event Horizon Telescope Collaboration, et al., 2022, ApJL, 930, L12
3. The Event Horizon Telescope Collaboration, et al., 2022, ApJL, 930, L14
4. Miyoshi, M., Kato, Y., & Makino, J. 2022, ApJ, 933, 36 https://iopscience.iop.org/article/10.3847/1538-4357/ac6ddb
5. Miyoshi, M., Kato, Y., & Makino, J. 2022, eprint arXiv:2207.13279 arXiv: arXiv:2207.13279 Bibcode:2022arXiv220713279M
6. Miyoshi, M., Kato, Y., Makino, J. & Tsuboi, M. 2024, ApJL, 963, L18 https://iopscience.iop.org/article/10.3847/2041-8213/ad250e
7. Miyoshi, M., Kato, Y., & Makino, J. 2024, MNRAS, accepted.